Forum Acusticum 2011 - Aalborg - Denmark

Ray-tracing modelling of the diffraction by half-planes based on the energy flow lines concept

Alexis Billon, Jean-Jacques Embrechts
University of Li, Li, Belgium

Abstract

Modelling diffraction within geometrical acoustics framework remains a challenge. Temporal and frequency models have been developed which can be time consuming and which are restricted to deterministic ray-paths (specular reflections). A diffraction model based on the Heisenberg uncertainty principle has been proposed recently [Stephenson, Acust. Acta Acust. (2010)]. This model can handle the diffusely reflected part of the energy, but it is known to be time consuming. Another diffraction model based on an approximation of the far-field direction of the Poynting vector has also been developed recently for the computation of scattering due to faceted dielectric objects [Hesse and Kulanowski, J. Quant. Spectrsc. Ra. (2003)]. Using the analogy between the Poynting and the acoustic intensity vectors, this model is implemented in this study within an acoustic ray-tracing software. In the vicinity of the diffracting edges, the rays are redirected according to their distance to the edge and the frequency. So, the proposed model can handle both diffuse and specular reflections and no limit is set in terms of reflection or diffraction order. Moreover, the additional calculation cost is very low. For an infinite half-plane, the results are in a good agreement with the uniform theory of diffraction.

PACS no. 43.55.Br, 43.55.Ka, 43.58.Ta

1. Introduction

In geometrical acoustics, sound propagation is assimilated to the propagation of rays carrying only acoustic power [1]. These models are very popular in room-acoustics due to their relatively low computation time compared to the more computationally intensive methods solving the wave equation. This is particularly important for (real-time) auralizations [2, 3] since these techniques require the calculation of room impulse responses.

However, they assume that energy travels along straight lines (for homogeneous propagation medium) and thus ignore the diffraction occurring at edges. To add these effects, two models are popular: the uniform theory of diffraction (UTD) [4, 5] and the Biot-Tolstoy-Medwin model (BTM) [6, 7, 8].

The UTD assumes an infinite diffracting edge and that both the source and the receiver are sufficiently far from the edge [4, 5]. Due to the low computing cost, this model has found several applications in room acoustics [9, 10]. On the other hand, the BTM permits a more detailed description of the problem and leads to more accurate results than the UTD, but at the expense of a computation time increase. The BTM also found some applications in room acoustics [11, 12].

One of the major problems to apply diffraction models to geometrical acoustics algorithms is the search for all the diffracted paths. If only specular reflections are considered, images of the diffracting edges onto the room's surfaces can be recursively constructed [11, 12]. However, each diffracting edge becomes a primary source in this method and the number of images to evaluate grows exponentially with the order of reflection, restricting the practical application to low reflection orders. Another method consists in tracing beams [9] or frustrums [10] from the sound source. Once discovered, these paths are used to propagate the energy from the source to the receiver.

In the preceding methods, the diffracted paths are only associated with specular reflections and the contributions of diffuse reflections are totally neglected. To allow for diffusely reflected energy being diffracted in ray-tracing algorithm, virtual surfaces extending the edges must be added such as they become visible by the propagating sound rays [13, 14, 15]. In these

models, each ray detecting the diffracting edge results in the emission of several tens of diffracted rays according to some defined directivity patterns. It results that these models are very computationally demanding.

Recently, a diffraction model [16] based on the direction of the energy flow lines [17] behind an infinite half-plane have been introduced to evaluate the scattering of light by ice crystals. The rays are deflected behind the edge depending on the approximated far field direction of the time-averaged Poynting's vector [17]. For perpendicular incident waves, a good agreement is analytically obtained with the rigorous Sommerfeld's solution [17].

In this paper, the energy flow lines diffraction model is extended to obliquely incident rays and implemented in an acoustic ray-tracing software. Comparisons with the UTD are then presented for an infinite half-plane.

2. Diffraction model

2.1. Rays in a plane perpendicular to the edge

The problem under consideration is the diffraction of plane waves propagating in a plane perpendicular to the edge by a half-plane (Fig. 1). For perpendicular incident waves (the incidence angle noted $\alpha = \pi/2$), Hesse and Ulanowski [16] proposed an empirical expression of the far field deflection angle of the energy flow lines given through the direction of the time-averaged Poynting's vector [17] behind the half-plane:

$$\phi(z) = -\arctan\frac{\lambda}{4\pi^2 z}, \tag{1}$$

where z is the distance between the passing plane waves and the diffracting edge and λ the wavelength. The concept assumes, similarly to the UTD [4, 5], that the edge is infinite and that both the source and the receptor are located far enough from the half-plane [16]. In acoustics, the Poynting's vector can be interpreted as the acoustic intensity vector [18] and the link with the acoustic ray-tracing algorithm is therefore straightforward.

Eq. 1 is very intuitive to interpret in geometrical acoustics: the closer of the diffracting edge the rays travel, the higher their deflection angle becomes, similarly to Stephenson's models [14, 15] (Figs. 2). The proposed concept deals only with energy quantities and cannot thus predict the phase jump occurring at the edge. On the other hand, the predicted field is intrinsically continuous at the shadow boundary.

For oblique incident waves, Eq. 1 can create some artifacts in the obtained diffracted field: If $\alpha < \pi/2$, the zone defined between $\phi = \pi/2$ and $\pi - \alpha$ cannot be reached by the diffracted rays and the acoustic field becomes discontinuous in the shadow zone (Fig. 3a).

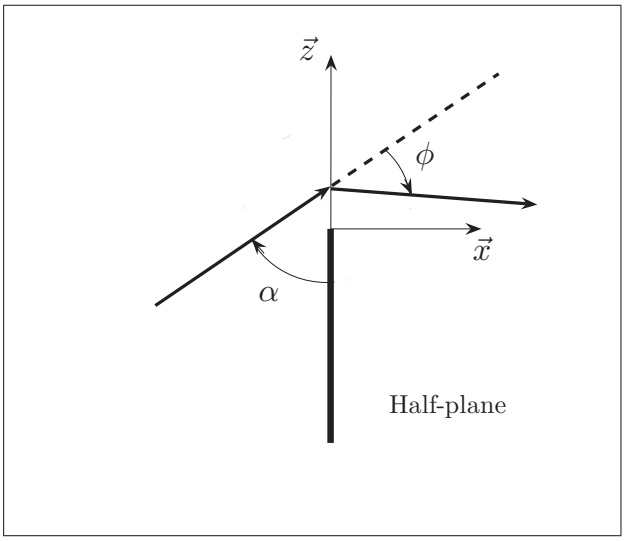

Figure 1. Plane wave incident on a half-plane. The wave vector is the plane perpendicular to the diffracting edge. α is the incidence angle comprised between 0 and π and ϕ is the deflection angle.

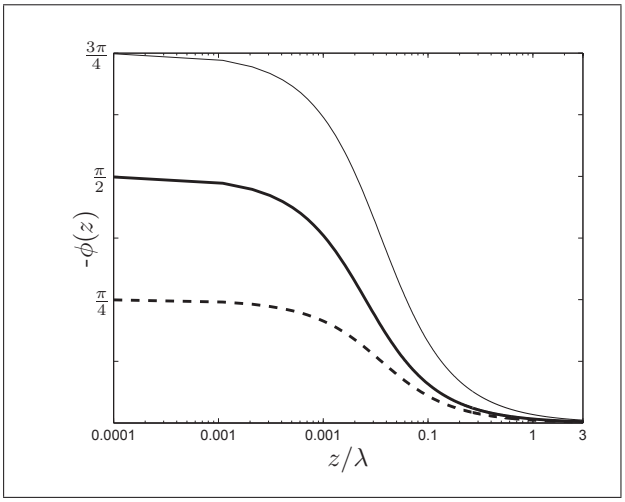

Figure 2. Evolution of the deflection angle -$\phi(z)$ obtained using Eq. 2 as a function of the edge-ray distance z/λ for an incidence angle α=$\pi/4$ (thin line), $\pi/2$ (bold line) and $3\pi/4$ (dashed line).

Similarly, if $\alpha > \pi/2$, the rays can be redirected in the lighted zone as reflected by the diffracting edge (Fig. 3b). So, the deflection angle must be bound by $\pi - \alpha$ and a correction factor is added to Eq. 1, such as:

$$\phi(z) = -2\frac{\pi - \alpha}{\pi}\arctan\frac{\lambda}{4\pi^2 z\sin\alpha}. \tag{2}$$

It should be noted that for α=$\pi/2$, Eq. 2 can be reduced to Eq. 1. Fig. 2 presents the obtained deflection angle computed with Eq. 2 as function of the edge-ray distance for an incidence angle α=$\pi/4$, $\pi/2$ and $3\pi/4$. For $\alpha = \pi/4$, the obtained diffraction angles cover the entirety of the shadow zone. The predicted energy flow lines are thus spread on a wider

(c) European Acoustics Association, ISBN: 978-84-694-1520-7, ISSN: 221-3767

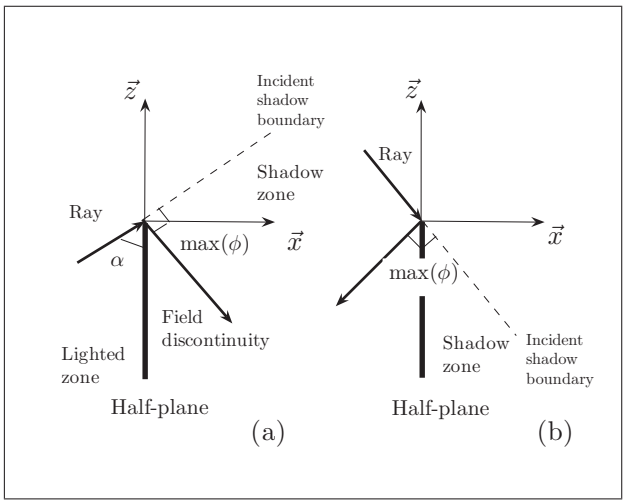

Figure 3. (a) Oblique incidence ray for $\alpha < \pi/2$ with the diffracted with maximal deflection evaluated using Eq. 1 ($\max(\phi) = \pi/2$). (b) Oblique incidence ray for $\alpha > \pi/2$ with the diffracted with maximal deflection evaluated using Eq. 1 ($\max(\phi) = \pi/2$).

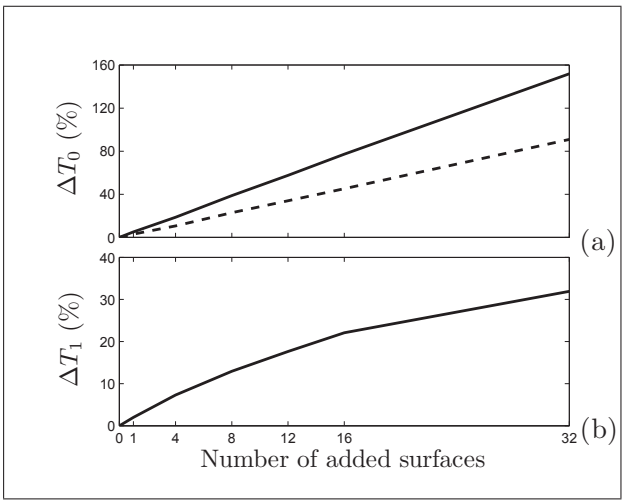

Figure 4. Evolution of the computation time as a function of the number of added surfaces. (a) ΔT_0 is evaluated in respect to the reference simulation with 38 surfaces: (thick line) the added surfaces are diffracting and (dashed line) the added surfaces are not diffracting. (b) ΔT_1 compares the simulations with diffraction to the ones without diffraction for the same number of surfaces.

angle compared to the perpendicular incident configuration. On the other hand, for $\alpha = 3\pi/4$, these lines are squeezed on a narrower angle. Both results seems physically consistent.

2.2. Rays in a plane oblique to the edge

If the incident wave propagates in a direction making an angle $\theta \neq \pi/2$ with the edge, the diffracted wave is conical [19]: the diffracted rays propagate along a cone oriented along the edge direction (noted down $\vec{e}$) and its aperture is equal to 2θ. Moreover, following Eq. 1, the diffracted ray must also lie in a deflection cone oriented along the incoming ray direction $\vec{r}$ and having an aperture equal to 2ϕ. So, the diffracted ray direction $\vec{s}$ must satisfy the following conditions:

$$\begin{cases} \cos\phi = \frac{\vec{s}\cdot\vec{r}}{|\vec{s}|\times|\vec{r}|} \\ \cos\theta = \frac{\vec{s}\cdot\vec{e}}{|\vec{s}|\times|\vec{e}|} \\ |\vec{s}| = 1 \end{cases} . \tag{3}$$

This system has two solutions: only ray deflected in the shadow zone is kept.

When the ray is perpendicular to the edge ($\theta = \pi/2$), the diffraction cone becomes a disc and the deflected ray can simply viewed as rotated around $\vec{e}$ about an angle ϕ.

2.3. Numerical implementation

To detect the possible deflected rays, each diffracting half-plane is topped by a virtual surface [13, 14, 15]. When the surface intersected by the the ray is a diffracting surface, its new direction must be evaluated. Then, the ray-tracing algorithm is continued as usual. During their flight time, the rays can be subjected to an unlimited number of reflections or diffractions. Moreover, the reflections can be diffuse or specular and can occur before or after the possible diffractions.

The main cost of the proposed diffraction concept is to add some virtual surfaces that increase the number of tested surfaces during the intersection test. On the other hand, the diffraction model remains independent of the chosen intersection algorithm and benefits of each of its improvement. As example, starting from a reference configuration with 38 surfaces, configurations with a number of diffracting surfaces varying from 1 to 32 are obtained (the geometrical models comprise then 39 to 70 surfaces). As a comparison, simulations are also performed where the diffracting surfaces are replaced by classical surfaces, without diffraction.

The first criterion investigated is ΔT_0 the relative increase of computation time with respect to the reference simulation (Fig. 4a). The computation time with the diffraction model increases linearly with the number of surfaces, as it is usual with ray-tracing algorithms. Compared to the configurations without diffraction model, the computation time increase ΔT_0 is about 50% with the diffraction model.

The simulations with and without diffraction can also be compared for the same number of surfaces through the criterion ΔT_1 (Fig. 4b). The increase of computation time can roughly be estimated to around 1% when one classical surface is replaced by a diffracting surface.

The ray-tracing algorithm is known to be prone to sampling issues [20]: the number of emitted rays is limited and some important propagation paths can be missed. The point is even more crucial in the pro-

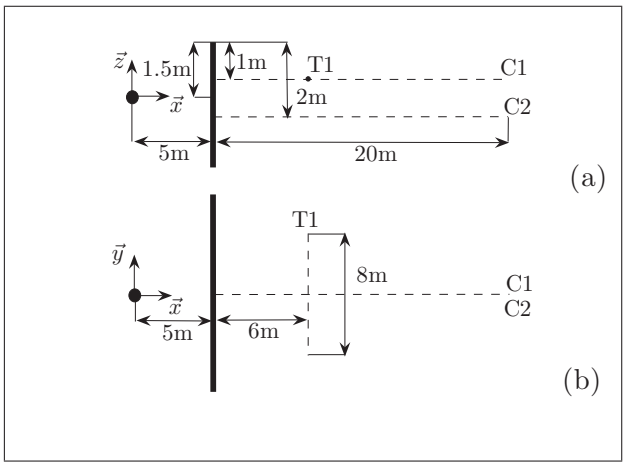

Figure 5. (a) Cross-section of the studied configuration and (b) top-view of the studied configuration.

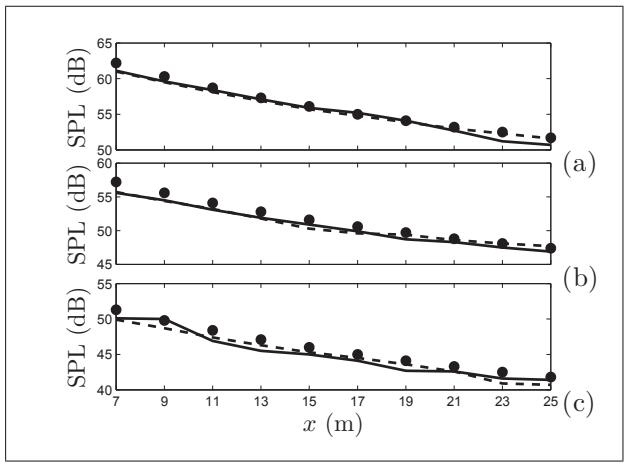

Figure 6. Evolution of the sound pressure level (SPL) along C1 at (a) 125Hz, (b) 500Hz and (c) 2000Hz: (•) uniform theory of diffraction, (thick line) ray-tracing with 10^7 rays and (dashed line) 10^8.

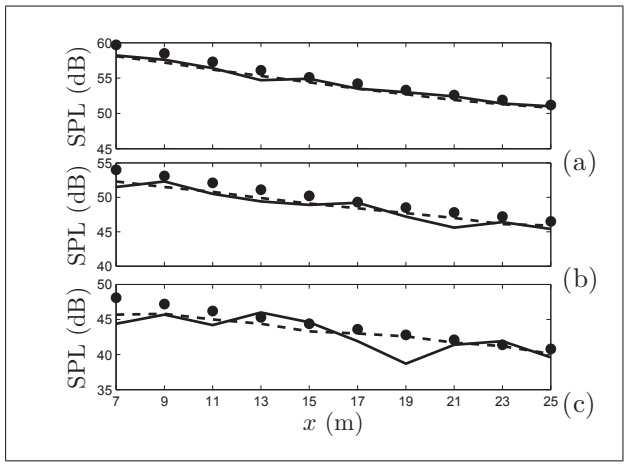

Figure 7. Evolution of the sound pressure level (SPL) along C2 at (a) 125Hz, (b) 500Hz and (c) 2000Hz: (•) uniform theory of diffraction, (thick line) ray-tracing with 10^7 rays and (dashed line) 10^8.

posed diffraction model. Fig. 2 shows that the deflection occurs mainly within the first wavelength over the diffracting edge. So, if the number of rays crossing the detection zone is too low, the shadow zone will be only loosely covered and some discontinuities may appear in the resulting diffracted field.

3. Validation

In this section, the ray-tracing results are compared with those obtained using the UTD. The studied configuration is presented in Fig. 5. The sound source is a point source with a sound power level of 100dB and three frequencies (125, 500 and 2000Hz) are considered.

The sound pressure level (SPL) is first measured behind the half-plane along two lines following the x axis: the line C1 is located 1m below the diffracting edge and the line C2 2m below (Fig. 5a). A third measurement line noted down T1 is parallel to the half-plane, following the y axis (Fig. 5b). For the ray-tracing simulations, 10^7 rays are emitted. The sound receivers are spherical with 0.5m diameter and located every 2m along C1 and C2 and every meter along T1. The computation time is about 60s.

The ray tracing's results are in a good agreement with those obtained with the UTD along C1, C2 and T1. The mean discrepancy is less than 2dB (Figs. 6-8). The proposed diffraction model tends to slightly underestimates the sound pressure level compared to the UTD. This underestimation is partly due to the empirical expression of Eq. 2 and partly to the statistical errors associated with the ray-tracing algorithm.

The deviation is thus greater closer to the half-plane and deeper in the shadow zone. This corresponds to the greatest deflection angles which are associated with passing distances less than 0.1λ (Fig. 2). Moreover, both the mean Er_m and the maximal Er_M discrepancies between the ray-tracing and the UTD increase with the frequency (Tab. I). This is also linked to the decreasing size of the effective surface redirecting the rays with increasing frequency. If this surface is approximated by a height equal to 3λ and considering the sound receiver diameter (0.5m), the effective solid angle starting from the source is evaluated to 0.098 Sr at 125Hz, 0.035 Sr at 500Hz and 0.009 Sr at 2000Hz. The number of rays passing through the effective diffracting surface can be then estimated to about 78.10^3 at 125Hz, 28.10^3 at 500Hz and 7.10^3 at 2000Hz. This decreasing number of redirected rays hitting the sound receivers (Fig. 9) can explain the under-sampling and the increased statistical error at high frequencies.

Increasing the number of emitted rays from 10^7 to 10^8 (and similarly increasing the computation time by a factor 10) has a marginal effect on the results obtained along C1 (Fig. 6) at every frequency and along C2 (Fig. 7) at 125Hz (Tab. II). In this case,

(c) European Acoustics Association, ISBN: 978-84-694-1520-7, ISSN: 221-3767

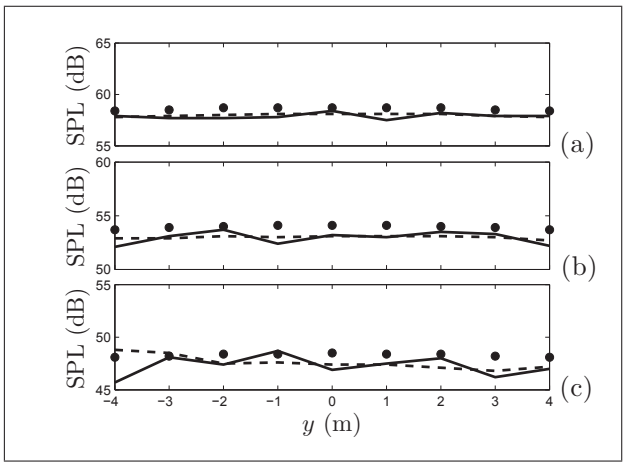

Figure 8. Evolution of the sound pressure level (SPL) along T1 at (a) 125Hz, (b) 500Hz and (c) 2000Hz: (•) uniform theory of diffraction, (thick line) ray-tracing with 10^7 rays and (dashed line) 10^8.

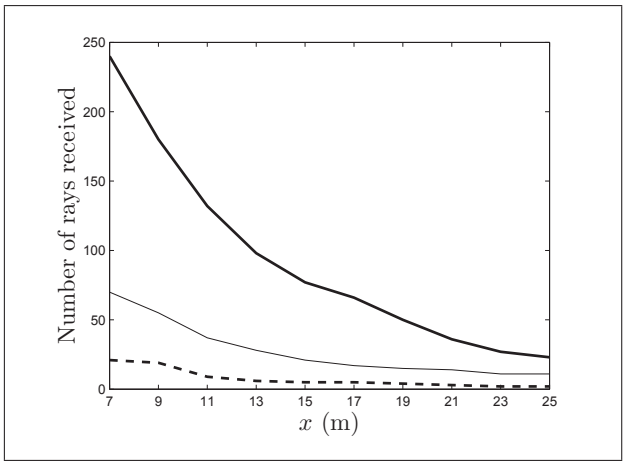

Figure 9. Evolution of the number of rays traversing the spherical sound receivers along the section C2: (thick line) 125Hz, (thin line) 500Hz and (dashed line) 2000Hz.

Table I. Mean (Er_m) and maximal (Er_M) discrepancies between the ray-tracing using 10^7 rays and the uniform theory of diffraction results for C1, C2 and T1.

	C1		C2		T1	
Hz	Er_m (dB)	Er_M (dB)	Er_m (dB)	Er_M (dB)	Er_m (dB)	Er_M (dB)
125	0.6	1.3	0.7	1.5	0.7	1.2
500	0.8	1.5	1.3	2.5	1.0	1.7
2000	1.0	1.6	1.6	4.1	0.7	2.4

the main source of discrepancy is due to the modeling of diffraction. On the other hand, the discrepancies along C2 are effectively reduced at 500Hz and 2000Hz and also at 2000Hz for the results along T1.

4. Conclusions

Geometrical acoustic models, approximating the sound waves propagation by rays carrying only energy information, are very popular in room-acoustics and auralization due to their low computation load. However, they seldom model diffraction effects, restricting their applications.

Table II. Mean (Er_m) and maximal (Er_M) discrepancies between the ray-tracing using 10^8 rays and the uniform theory of diffraction results for C1, C2 and T1.

	C1		C2		T1	
Hz	Er_m (dB)	Er_M (dB)	Er_m (dB)	Er_M (dB)	Er_m (dB)	Er_M (dB)
125	0.4	1.2	0.9	1.6	0.6	0.7
500	0.9	1.6	1.1	1.7	1.0	1.1
2000	0.9	1.6	0.9	2.4	0.9	1.4

In this paper, a diffraction model developed to predict the scattering of light by ice crystals is adapted to an acoustic ray-tracing software. To simulate diffraction by half-planes, the rays passing in the vicinity of the diffracting edges are deflected in the shadow zone depending on the ray-edge distance and on the frequency. The deflection law is based on an approximation of the far field direction of the time averaged Poynting's vector. This model considers an infinite edge and that the source and the receiver are far enough from the diffracting edge. This model is here extended to obliquely incident rays and compared with the uniform theory of diffraction.

For a half-plane, the obtained results are in a good agreement with the uniform theory of diffraction for the tested frequencies and locations. The observed discrepancies are due to the approximated deflection law and to sampling issues related to the size of the detecting surface. Moreover, the obtained predictions are more reliable at lower frequencies for a given number of rays.

The computation load grows linearly with the number of diffracting edges, similarly to a classical ray-tracing algorithm. Each diffracting surface increases the computation time by an amount of 1 %, if the total number of surfaces is kept constant. Moreover, the proposed model is only a variation of the ray-tracing algorithm and is compatible with most of ray-tracing accelerating techniques.

Further work must be done to improve the presented diffraction algorithm. The diffraction model is restricted to diffraction around half-planes and must be extended to wedges of arbitrary angle and slits.

Acknowledgement

Alexis Billon wishes to thank the *Fonds de la Recherche Scientifique* (FNRS) for providing financial support to this work (Grant 2.4.534.09.F).

References

[1] H. Kuttruff: Room acoustics 4th ed., Taylor & Francis, London, 2000.

[2] M. Kleiner, B-I. Dalenb, UP. Svensson: Auralization an overview. J. Audio Eng. Soc. **41** (1993) 861875.

[3] M. Vorler: Auralization, Springer, Berlin 2007.

[4] G. Kouyoumjian, P. Pathak: A uniform geometrical theory of diffraction for an edge in a perfectly conducting surface. Proc. 1974 IEEE, 1448-1461.

[5] DA. McNamara, CWI. Pistorius, JAG. Malherbe: Introduction to the uniform geometrical theory of diffraction. Artec House, New York, 1990.

[6] MA. Biot, I.Tolstoy: Formulation of wave propagation in infinite media by normal coordinates with an application to diffraction. J. Acous. Soc. Am. **29** (1957) 381-391.

[7] H. Medwin: Shadowing by finite noise barriers. J. Acous. Soc. Am. **69** (1981) 1060-1064.

[8] UP. Svensson, RI. Fred, J. Vanderkooy: An analytic secondary source model of edge diffraction impulse responses. J. Acous. Soc. Am. **106** (1999) 2331-2344.

[9] N. Tsingos, T. Funkhouse, A. Ngan, I. Carlbom: Modeling acoustics in virtual environments using the Uniform Theory of Diffraction. Proc. 2001 ACM Computer Graphics (SIGGRAPH01), 545552.

[10] A. Chandak, C. Lauterbach, M. Taylor, Z. Ren, D. Manocha: ADFrustum: Adaptive frustum tracing for interactive sound propagation. EEE T. Vis. Comput. Gr. **14** (2008) 17071722.

[11] V. Pulkki, T. Lokki, L. Savojia: Implementation and visualization of edge diffraction with image-source method. Preprint 5603 in 112th AES Convention, 2002.

[12] D. Schrder, A. Pohl: Real-time hybrid simulation method including edge diffraction. Proc. of the EAA Symposium on Auralization 2009, 1-6.

[13] G. Benedetto, R. Spagnolo: A study of barriers in enclosures by a ray-tracing computer model. Acustica **17** (1984) 183-199.

[14] U. Stephenson: An energetic approach for the simulation of diffraction with ray tracing based on the uncertainty relation. Acust. Acta Acust. **96** (2010) 516-535.

[15] U. Stephenson: An analytically derived sound particle diffraction model. Acust. Acta Acust. **96** (2010) 1051-1068.

[16] E. Hesse, Z. Ulanowski: Scattering from long prisms computed using ray tracing combined with diffraction facets. J. Quant. Spectrosc. Ra. **79-80** (2003) 721-732.

[17] M. Born, E. Wolf: Principles of optics, 3rd ed., Pergamon Press, 1965.

[18] A. Pierce: Acoustics: An introduction to its physical principles and applications. Acoustical Society of America, 1989.

[19] J. Keller: Geometrical theory of diffraction. J. Opt. Soc. Am. **52** (1962) 116-130.

[20] H. Lehnert: Systematic errors of ray-tracing algorithm. Appl. Acoust. **38** (1993) 207-221.